



Arterial ^{18}F -Fluorodeoxyglucose Uptake Reflects Balloon Catheter-Induced Thrombus Formation and Tissue Factor Expression via Nuclear Factor- κB in Rabbit Atherosclerotic Lesions

Atsushi Yamashita, MD, PhD; Yan Zhao, MD, PhD; Songji Zhao, MD, PhD; Yunosuke Matsuura, MD; Chihiro Sugita, BSc; Takashi Iwakiri, MD; Nozomi Okuyama, BSc; Kazuyo Ohe, PhD; Chihiro Koshimoto, PhD; Keiichi Kawai, PhD; Nagara Tamaki, MD, PhD; Yuji Kuge, PhD; Yujiro Asada, MD, PhD

Background: Imaging modalities to assess atherosclerotic plaque thrombogenicity have not been established, so in this study the relationship between [^{18}F]-fluorodeoxyglucose (^{18}F -FDG) uptake and thrombus formation was investigated in rabbit atherosclerotic arteries.

Methods and Results: Atherosclerotic plaque was induced in the iliacofemoral artery by balloon injury and a 0.5% cholesterol diet. At 3 weeks after the first balloon injury, the arteries were visualized by ^{18}F -FDG positron emission tomography (PET) imaging 2h after an ^{18}F -FDG infusion, and then arterial thrombus was induced by a second balloon injury of both iliacofemoral arteries. Imaging with ^{18}F -FDG-PET revealed significantly more radioactivity along the injured (0.63 ± 0.12 SUVmax), than the contralateral non-injured artery (0.34 ± 0.08 SUVmax, $n=17$, $P<0.0001$). Arterial radioactivity measured by autoradiography positively correlated with macrophage area, the number of nuclei that were immunopositive for nuclear factor κB (NF- κB), and tissue factor (TF) expression. The immunopositive areas for glycoprotein IIb/IIIa and fibrin in thrombi were significantly larger in the atherosclerotic than in the contralateral arteries, and significantly correlated with radioactivity in PET ($r=0.92$, $P<0.001$, $n=10$) and autoradiography ($r=0.73$, $P<0.0001$, $n=50$) in the arteries. Inhibition of NF- κB significantly reduced TF expression in cultured atherosclerotic plaque.

Conclusions: Arterial ^{18}F -FDG uptake reflects the thrombogenicity of atherosclerotic plaque following balloon injury.

Key Words: Atherothrombosis; ^{18}F -FDG; Nuclear factor- κB ; Rabbits; Tissue factor

Thrombus formation is a major complication of atherosclerosis, but although disruption of atherosclerotic plaques is recognized as a trigger of atherothrombosis, not all thrombi result in complete luminal occlusion and symptomatic events.^{1,2} Therefore, thrombus size is critical to the onset of clinical events. Thrombus formation and propagation are regulated by many factors, such as vascular wall thrombogenicity, local hemorheology, blood thrombogenicity, and fibrinolytic activity.³ Among these, the thrombogenicity of ath-

erosclerotic plaque is an essential factor in atherothrombosis. Tissue factor (TF) is an initiator of the coagulation cascade that is expressed in the adventitia and to various degrees in the media of normal arteries.⁴ Because atherosclerotic plaques express TF, the degree of TF expression is a crucial determinant of plaque thrombogenicity.⁵ Although current imaging modalities support high-quality plaque characterization,⁶ those that can assess atherosclerotic plaque thrombogenicity have not been established.

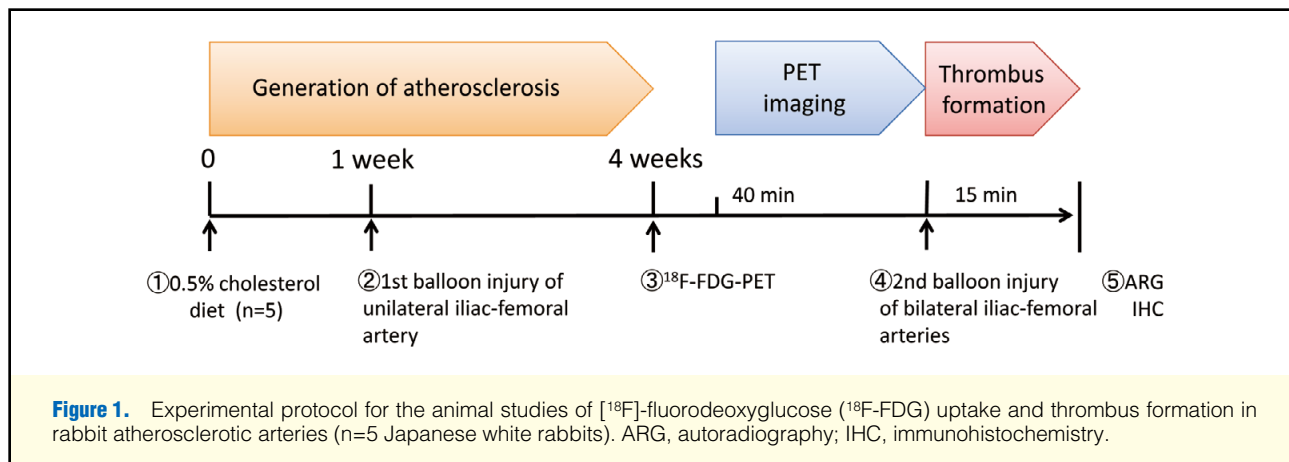
Received November 27, 2012; revised manuscript received April 22, 2013; accepted May 23, 2013; released online July 6, 2013 Time for primary review: 29 days

Department of Pathology (A.Y., Y.M., C.S., T.I., N.O., Y.A), Department of Internal Medicine (Y.M., T.I.), Department of Faculty of Medicine, Frontier Science Research Center (C.K.), University of Miyazaki, Miyazaki; Department of Tracer Kinetics & Bioanalysis (Y.Z., S.Z.), Department of Nuclear Medicine (N.T.), Graduate School of Medicine, Central Institute of Isotope Science (Y.K.), Hokkaido University, Sapporo; Faculty of Health Sciences, Institute of Medical, Pharmaceutical and Health Sciences, Kanazawa University, Ishikawa (K.O., K.K.); and Biomedical Imaging Research Center, University of Fukui, Fukui (K.K.), Japan

Mailing address: Yujiro Asada, MD, PhD, Department of Pathology, Faculty of Medicine, University of Miyazaki, 5200 Kihara, Kiyotake, Miyazaki 889-1692, Japan. E-mail: yasada@med.miyazaki-u.ac.jp

ISSN-1346-9843 doi:10.1253/circj.CJ-12-1463

All rights are reserved to the Japanese Circulation Society. For permissions, please e-mail: cj@j-circ.or.jp



Positron emission tomography (PET) imaging using [¹⁸F]-fluorodeoxyglucose (¹⁸F-FDG) has been advocated as a means of evaluating arterial inflammation.⁷ The uptake of ¹⁸F-FDG closely correlates with plaque macrophage contents in animal models,^{8–10} which suggests that the degree of ¹⁸F-FDG accumulation in the vessel wall reflects underlying levels of inflammation. Clinical studies have also identified a relationship between ¹⁸F-FDG uptake and numbers of cardiovascular risk factors, as well as risk for future events.^{11–13} The uptake of ¹⁸F-FDG is significantly higher in aortic segments with, than without thrombus in a rabbit model of advanced atherosclerosis.¹⁴ These lines of evidence imply an association between ¹⁸F-FDG uptake and arterial thrombus formation, although the underlying mechanism is unknown. We investigated this notion in a rabbit model of atherosclerosis.

Methods

Experimental Protocol

The Animal Care Committee of Miyazaki University and Hokkaido University approved the animal research protocols of the present study, which also conformed to the Guide for the Care and Use of Laboratory Animals published by the US National Institutes of Health.

Figure 1 shows the experimental protocol of the ¹⁸F-FDG-PET study. The 5 male Japanese white rabbits weighing 2.5–3.0 kg were fed with a 0.5% cholesterol diet, and the iliofemoral artery was injured with a balloon catheter to induce atherosclerotic lesions. At 3 weeks after the first balloon injury, ¹⁸F-FDG-PET imaging proceeded 2 h after ¹⁸F-FDG infusion. Arterial thrombus was induced by a second balloon injury to both iliofemoral arteries and 15 min later, the amount of radioactivity in the arteries was evaluated and the arteries were immunohistochemically analyzed.

Atherosclerosis and Thrombosis Model

Surgery proceeded under aseptic conditions and general anesthesia was achieved via an intravenous injection of pentobarbital (25 mg/kg). At 1 week after feeding with a 0.5% cholesterol diet, an angioplasty balloon catheter (diameter, 2.5 mm; length, 9 mm; Quantum, Boston Scientific, Galway, Ireland) was inserted using a 4F introducer sheath (Goodman, Nagoya, Japan) via the carotid artery into the right iliofemoral artery under fluoroscopic guidance to induce an atherosclerotic lesion in the artery. The catheter was inflated to 1.5 atm (balloon-to-artery ratio; 1.1:1 to 1.2:1) and retracted 3 times to denude the

endothelium.

After ¹⁸F-FDG-PET imaging, a 2F balloon catheter (Baxter Healthcare) was inserted via the anterior tibial arteries into both iliofemoral arteries, inflated to 1.4 atm, and retracted twice to induce arterial thrombus;¹⁵ 15 min later, the rabbits were injected with heparin (500 U/kg, i.v.) and then killed 5 min later with an overdose of pentobarbital (60 mg/kg, i.v.). The animals were perfused with 50 ml of cold 0.01 mol/L of phosphate-buffered saline to remove residual blood from the arteries for subsequent autoradiography and immunohistochemical evaluation.

PET Imaging and Analysis

¹⁸F-FDG-PET imaging proceeded as described with minor modifications.¹⁶ The rabbits (n=5) were fasted for 4 h prior to PET scanning, infused with ¹⁸F-FDG (average, 193 MBq/rabbit) 2 h prior to imaging, and anesthetized by 1.5–2.0% isoflurane inhalation. The injected dose of ¹⁸F-FDG was determined in consideration of the half-life of ¹⁸F (110 min). After urinary bladder lavage with warmed saline, the rabbits were placed supine on a customized acrylic bed in a small animal PET scanner (Inveon, Siemens Medical Solutions USA, Knoxville, TN, USA) and scanned (list-mode acquisition) for 40 min. Body temperature (37.4±0.2°C) was maintained using cotton bedding prepared during the PET scanning. The data were reconstructed and corrected for attenuation and scatter using 2D filtered back-projection (FBP) and maximum a posteriori (MAP) algorithm. The spatial resolution was 1.63 mm full-width at half-maximum (FWHM) in FBP and 1.05 mm FWHM in MAP. The former was used to quantify the radioactivity and the latter for visual observations. The image matrix was 256×256×159, resulting in a voxel size of 0.385×0.385×0.796 mm. Coronal, axial and sagittal images were visually graded. Coronal images were quantified by centering regions of interest (ROIs) over the iliofemoral arteries, then 3 or 4 circular ROIs (10 pixels in diameter) in the FBP images were placed on each injured and contralateral non-injured artery. The results are expressed as standardized uptake value (SUV). The maximum values of SUV (SUVmax) for the bilateral arteries were confirmed and represented the ¹⁸F-FDG uptake in the PET images.

Radioactivity of Tissue and Arterial Slices

The amount of radioactivity in the iliofemoral arteries, skeletal muscle tissue, and blood was measured using a well-type γ -counter (1480 Wizard 3; Wallac Co Ltd, Turku, Finland). The results are calculated as (%ID/g)×kg and then converted

to SUV.¹⁷

The arteries were cut into 5 sections that were embedded in Tissue-Tek (Sakura, Tokyo, Japan) and frozen. Consecutive 10- or 5- μm slices were prepared for autoradiographic or histologic analysis, respectively. The 10- μm cryostat sections were exposed to phosphor imaging plates (Fuji Imaging Plate BAS-SR 2025, Fuji Photo Film Co Ltd, Tokyo, Japan) for 12h, together with a set of calibrated standards.⁸ The imaging plates were then scanned using a Fuji Bio-imaging Analyzer BAS-5000 with an internal resolution of 25 μm (Fuji Photo Film Co Ltd) and the images were examined using image analysis software (Multi Gauge Ver. 3.0, Fuji Photo Film Co Ltd). The amount of radioactivity in each image is expressed as photostimulated luminescence per unit area ($\text{PSL}=\text{a}\times\text{D}\times\text{t}$, where a is a constant, D is the amount of radioactivity exposed on the image plate, and t is exposure time). Each PSL value/ mm^2 of arterial tissue was recorded and converted to a ratio (%) of the activity of the standard injected dose/ mm^2 of lesion area (% ID/ mm^2). The data were normalized with the animal's body weight (%ID \times kg/ mm^2) and then converted to SUV.¹⁸

Histologic Analysis

Consecutive 5- μm slices were fixed in acetone, stained with hematoxylin–eosin, and immunohistochemically examined using antibodies against muscle actin (HHF35, Dako, Glostrup, Denmark), rabbit macrophages (RAM11, Dako), CD163 (AM-3K, Trans Genic Inc, Kobe, Japan), nuclear factor κB (NF- κB ; Abnova, Taipei, Taiwan), TF (mouse IgG2b subclass for rabbit TF extracellular domain (193Ser-207Cys)), glycoprotein (GP) IIb-IIIa (Affinity Biologicals Inc, Hamilton, CA, USA) and rabbit fibrin (Takeda Chemical Industries Ltd, Osaka, Japan). The sections were stained with Envision (Dako) or donkey anti-sheep IgG secondary antibody (Jackson ImmunoResearch, Baltimore, MA, USA). Horseradish peroxidase activity was visualized using 3, 3'-diaminobenzidine tetrahydrochloride, and counterstained with Meyer's hematoxylin. Immunostaining controls included non-immune mouse IgG or non-immune sheep serum instead of the primary antibodies. Areas of positive immunostaining in the vessel and thrombus were analyzed using a color imaging morphometry system (Win Roof, Mitani, Fukui, Japan).¹⁵ The data are expressed as ratios of the immunopositive area (μm^2), or as numbers of immunopositive nuclei/ mm^2 .

For double immunofluorescence, antibodies for rabbit macrophage (RbM2, TransGenic Inc) and smooth muscle actin (SMA; 1A4, Novus Biologicals, Littleton, CA, USA) were labeled with Mix-n-Stain CF594 antibody labeling kit (Biotium, Hayward, CA, USA). The sections were stained with CF488A labeled secondary antibody (Biotium) for NF- κB and CF594-labeled antibodies for rabbit macrophages or SMA.

Tissue Culture of Rabbit Atherosclerotic Plaque

Atherosclerotic lesions were induced as described. The rabbits were injected with heparin (500 U/kg, i.v.), killed 5 min later with an overdose of pentobarbital (60 mg/kg, i.v.) and perfused with 50 ml of 0.01 mol/L of phosphate-buffered saline and Dulbecco's modified Eagle's medium. The iliofemoral artery was excised and the atherosclerotic plaque was separated from the media and adventitia. The plaque was divided into 3-mm segments and placed in incubation medium containing 10% fetal bovine serum in multidishes for 6h. Cell viability was evaluated in plaque segments stained with nicotinamide adenine dinucleotide-hydrogen (NADH) and nitro blue tetrazolium. The plaque segments (n=5) were frozen before or 6h after incubation, and then 5- μm sections were incubated at 37°C for

1h in 10 ml of Gomeri Tris-HCl buffer (pH 7.4) containing 24 mg of nitroblue tetrazolium (Nacalai Tesque, Kyoto, Japan) and 10 mg of NADH (CalBiochem, San Diego, CA, USA).¹⁹ The amount of TF protein in plaque segments was measured using a rabbit TF ELISA kit (Uscn Life Science Inc, Wuhan, China) before and at 6h after incubation with Bay 11-7085 (an inhibitor of inhibitor of κB kinase, Merck, Darmstadt, Germany) or dimethyl sulfoxide.

Statistical Analysis

All data are presented as means and standard deviation. Differences between individual groups were tested using the Mann-Whitney U-test (GraphPad Prism 4.03, GraphPad Software Inc, San Diego, CA, USA). Relationships between factors were evaluated using Spearman's rank correlation coefficient and $P<0.05$ was considered statistically significant.

Results

PET Imaging and Radioactivity of Arteries

Figure 2 shows the ^{18}F -FDG-PET coronal MAP image and radioactivity accumulation before arterial thrombus formation. The accumulation of ^{18}F -FDG is greater along the injured than the non-injured artery (**Figure 2A**). We compared ^{18}F -FDG uptake between the injured and non-injured arteries by analyzing coronal FBP images after drawing ROIs centered over the iliofemoral arteries. The maximal amount of radioactivity in the ROIs was significantly higher in the injured than in the non-injured arteries (0.63 ± 0.12 vs. 0.34 ± 0.08 SUV_{max}; n=17, $P<0.0001$; **Figure 2B**). Significantly more radioactivity was found in the excised injured but not the non-injured iliofemoral artery (1.32 ± 0.55 vs. 0.35 ± 0.11 SUV_{mean}; n=5, $P<0.01$; **Figure 2C**). **Figure 2D** shows that level of ^{18}F -FDG uptake correlated between PET image and tissue ($r=0.71$, $P<0.05$; n=10). Levels of ^{18}F -FDG uptake were similar among the non-injured artery, blood and skeletal muscle tissue (0.35 ± 0.11 , 0.28 ± 0.05 and 0.37 ± 0.24 SUV, respectively; mean, n=5).

Autoradiographic and Histologic Findings

Figures 3A and **3B** shows the autoradiographic and histologic images of the injured and non-injured arteries with thrombi. Significantly more radioactivity was found in sections of the injured than the non-injured artery (7.96 ± 3.84 vs. 1.05 ± 0.93 SUV mean, n=25; $P<0.0001$). We evaluated cellular components, inflammatory response, vascular wall thrombogenicity and thrombus content by immunohistochemical staining for muscle actin, RAM11 (macrophage), CD163 (M2 macrophage marker), NF- κB , TF, GPIIb/IIIa and fibrin. The cellular composition at 3 weeks before injured arteries was rich in macrophages with smooth muscle cells (SMCs) (ie, atherosclerotic), whereas that in the contralateral artery mainly comprised SMCs with a few macrophages in the adventitia (**Figures 3A,B**). The CD163-immunopositive area accounted for 0.2% in the atherosclerotic arteries. The ratio of CD163 positive area to RAM11 positive area was 0.01. The ratio of immunopositive areas for muscle actin and macrophages to vascular area was significantly smaller and larger, respectively, in the atherosclerotic than in the contralateral arteries (**Figure 3B**).

Thrombi that developed within 15 min of balloon injury comprised platelets and fibrin (**Figure 3A**). More areas were immunopositive for GPIIb/IIIa and/or fibrin in the atherosclerotic (GPIIb/IIIa, 0.030 ± 0.019 mm^2 ; fibrin, 0.021 ± 0.019 mm^2 ; GPIIb/IIIa+fibrin, 0.052 ± 0.035 mm^2) than in the contralateral (GPIIb/IIIa, 0.010 ± 0.002 mm^2 ; $P<0.0001$, n=25; fibrin, 0.005 ± 0.003 mm^2 ; $P<0.0001$, n=25; GPIIb/IIIa+fibrin, $0.010\pm$

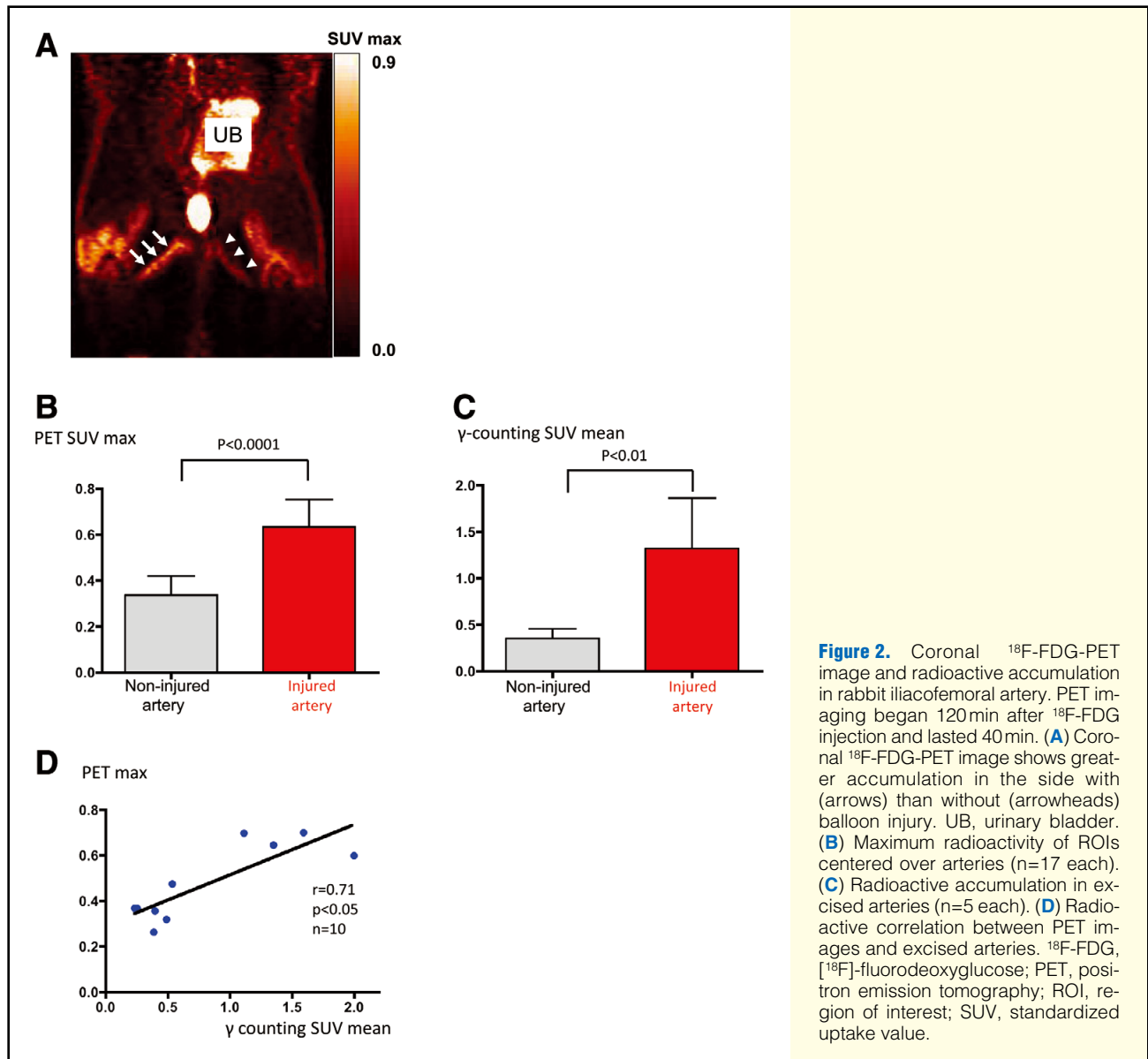


Figure 2. Coronal ^{18}F -FDG-PET image and radioactive accumulation in rabbit iliofemoral artery. PET imaging began 120 min after ^{18}F -FDG injection and lasted 40 min. **(A)** Coronal ^{18}F -FDG-PET image shows greater accumulation in the side with (arrows) than without (arrowheads) balloon injury. UB, urinary bladder. **(B)** Maximum radioactivity of ROIs centered over arteries ($n=17$ each). **(C)** Radioactive accumulation in excised arteries ($n=5$ each). **(D)** Radioactive correlation between PET images and excised arteries. ^{18}F -FDG, [^{18}F]-fluorodeoxyglucose; PET, positron emission tomography; ROI, region of interest; SUV, standardized uptake value.

0.003 mm², $P<0.0001$; $n=25$) arteries (**Figure 3B**).

Immunoreactivity for NF- κ B and TF was mainly localized in the macrophage-rich area in the atherosclerotic artery (**Figure 4A**). Double immunofluorescence showed NF- κ B-immunopositive nuclei in macrophages and SMCs (**Figure 4B**). The ratio of macrophage to NF- κ B-positive nuclei ($69\pm 13\%$, $n=13$) was more than the ratio of SMCs to them ($26\pm 9\%$, $n=13$, $P<0.0001$). Immunopositive nuclei for NF- κ B and the immunopositive area for TF were greater in the atherosclerotic (NF- κ B: $208\pm 225/\text{mm}^2$, TF: $4.7\pm 3.3\%$) than in the contralateral (NF- κ B, $22\pm 33/\text{mm}^2$, $P<0.0001$, $n=25$; TF, $0.4\pm 0.4\%$, $P<0.0001$, $n=25$) artery (**Figure 4C**). In addition, the number of NF- κ B positive nuclei and TF immunopositive areas significantly correlated ($r=0.63$, $P<0.0001$, $n=50$; **Figure 4C**).

Correlation Between ^{18}F -FDG Uptake and Histologic Findings

Figure 5 shows the correlation between ^{18}F -FDG uptake and vascular/thrombus factors. Autoradiographic ^{18}F -FDG uptake positively correlated with areas that were immunopositive

(%) for macrophages ($r=0.71$, $P<0.0001$, $n=50$), TF ($r=0.64$, $P<0.0001$, $n=50$), and the number of NF- κ B ($r=0.85$, $P<0.0001$, $n=50$), and negatively with SMCs ($r=-0.44$, $P<0.01$, $n=50$) (**Figure 5A**). The ^{18}F -FDG uptake also positively correlated with areas that were immunopositive for GPIIb/IIIa ($r=0.77$, $P<0.0001$, $n=50$), fibrin ($r=0.66$, $P<0.0001$, $n=50$), GPIIb/IIIa and fibrin ($r=0.73$, $P<0.0001$, $n=50$; **Figure 5B**). In addition, maximal ^{18}F -FDG uptake in PET images positively correlated with areas that were immunopositive for GPIIb/IIIa ($r=0.82$, $P<0.01$, $n=10$), fibrin ($r=0.95$, $P<0.001$, $n=10$), GPIIb/IIIa and fibrin ($r=0.92$, $P<0.001$, $n=10$; **Figure 5C**).

TF Expression in Tissue Cultures of Atherosclerotic Plaque

We assayed cultured plaques to determine the associations between NF- κ B and TF expression in rabbit atherosclerotic lesions. Atherosclerotic lesions were cut into 2-mm sections and cultured in conditioning medium with 10% FBS. The number of NF- κ B-immunopositive nuclei and the TF protein levels in the plaques were significantly increased 6 h later, compared with before plaque culture. Inhibiting NF- κ B using Bay

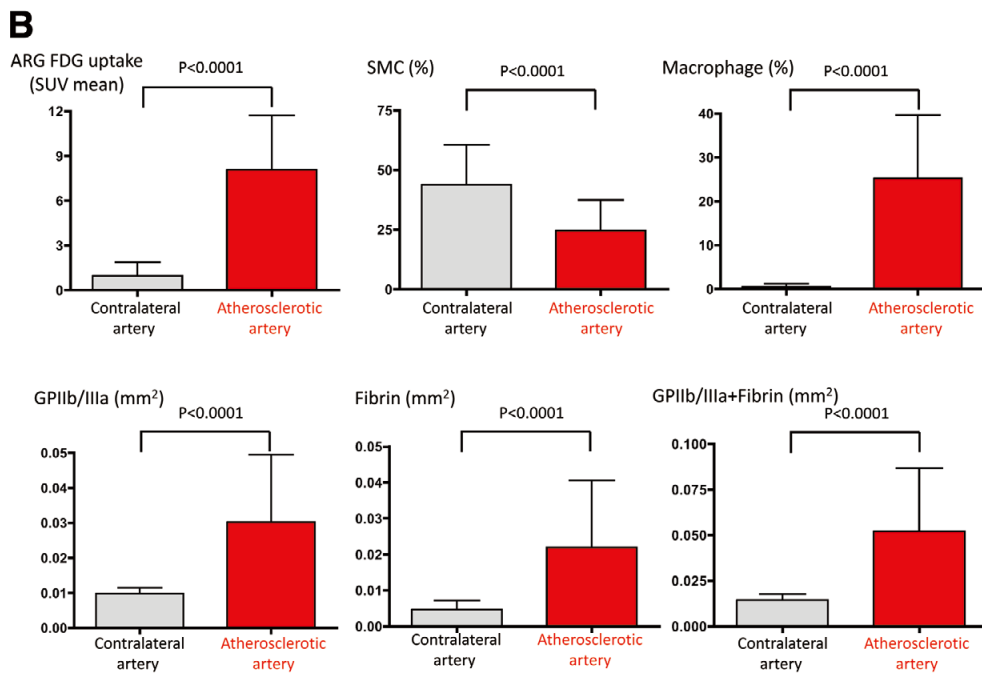
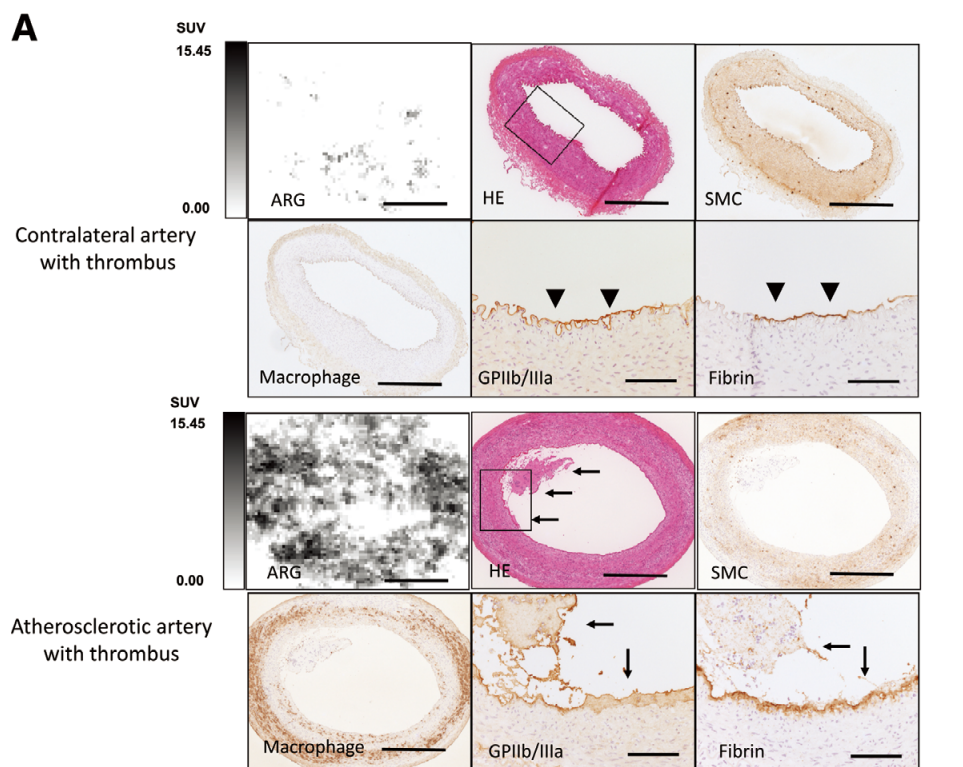


Figure 3. Autoradiographic (ARG) and histologic findings of atherosclerotic (injured) and contralateral (non-injured) arteries with thrombus in rabbits fed with 0.5% cholesterol diet. **(A)** Representative autoradiogram (HE stain), and immunohistochemistry for muscle actin, rabbit macrophage, GPIIb/IIIa, and fibrin. Immunoreaction is visualized by 3, 3'-diaminobenzidine tetrahydrochloride (brown). Uptake of ¹⁸F-FDG is low in the contralateral artery (**Upper**) comprising smooth muscle cells (SMCs) and some macrophages and a thin layer of mural thrombus comprising platelets and fibrin (arrowheads) covers the luminal surface. Uptake of ¹⁸F-FDG is high in atherosclerotic artery (lower rows) that is rich in macrophages. A thicker layer of mural thrombus comprising platelets and fibrin (arrows) covers the luminal surface. Immunohistochemical images of GPIIb/IIIa and fibrin correspond to square frames in the HE images. Bars=500 μm (ARG, HE, SMC, Macrophage) or 100 μm (GPIIb/IIIa and fibrin). **(B)** Uptake of ¹⁸F-FDG and immunopositive areas for muscle actin, macrophages, GPIIb/IIIa, fibrin, and GPIIb/IIIa and fibrin in arterial sections (n=25 each). ¹⁸F-FDG, [¹⁸F]-fluorodeoxyglucose.

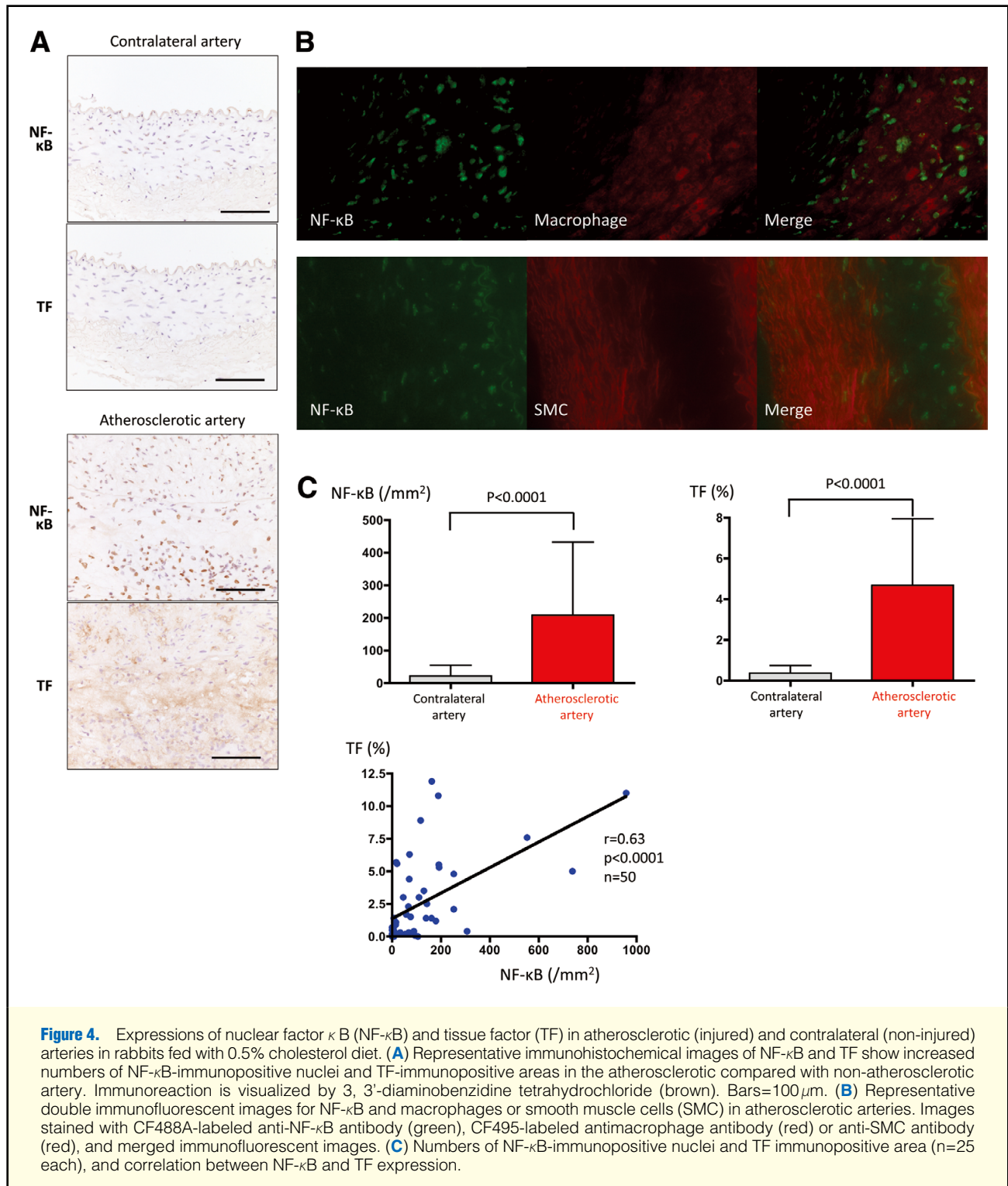


Figure 4. Expressions of nuclear factor κ B (NF- κ B) and tissue factor (TF) in atherosclerotic (injured) and contralateral (non-injured) arteries in rabbits fed with 0.5% cholesterol diet. **(A)** Representative immunohistochemical images of NF- κ B and TF show increased numbers of NF- κ B-immunopositive nuclei and TF-immunopositive areas in the atherosclerotic compared with non-atherosclerotic artery. Immunoreaction is visualized by 3, 3'-diaminobenzidine tetrahydrochloride (brown). Bars=100 μ m. **(B)** Representative double immunofluorescent images for NF- κ B and macrophages or smooth muscle cells (SMC) in atherosclerotic arteries. Images stained with CF488A-labeled anti-NF- κ B antibody (green), CF495-labeled antimacrophage antibody (red) or anti-SMC antibody (red), and merged immunofluorescent images. **(C)** Numbers of NF- κ B-immunopositive nuclei and TF immunopositive area (n=25 each), and correlation between NF- κ B and TF expression.

11-7055, an inhibitor of inhibitor of κ B kinase, significantly reduced both the number of NF- κ B-immunopositive nuclei (Figure 6A) and TF protein production (Figure 6B). Staining for NADH did not significantly differ among the groups (before culture, $40.4 \pm 8.7\%$; 6h after culture with DMSO and with Bay 11-7055, $43.2 \pm 10.6\%$ and $46.8 \pm 5.0\%$, respectively; n=5 each).

Discussion

The main findings of the present study are presented. Significantly more ^{18}F -FDG was taken up and more thrombus formed in the injured than in the non-injured arteries, and ^{18}F -FDG uptake significantly correlated with thrombus size, NF- κ B immunopositive nuclei and TF expression in the arteries. The inhibition of NF- κ B significantly reduced TF expression in

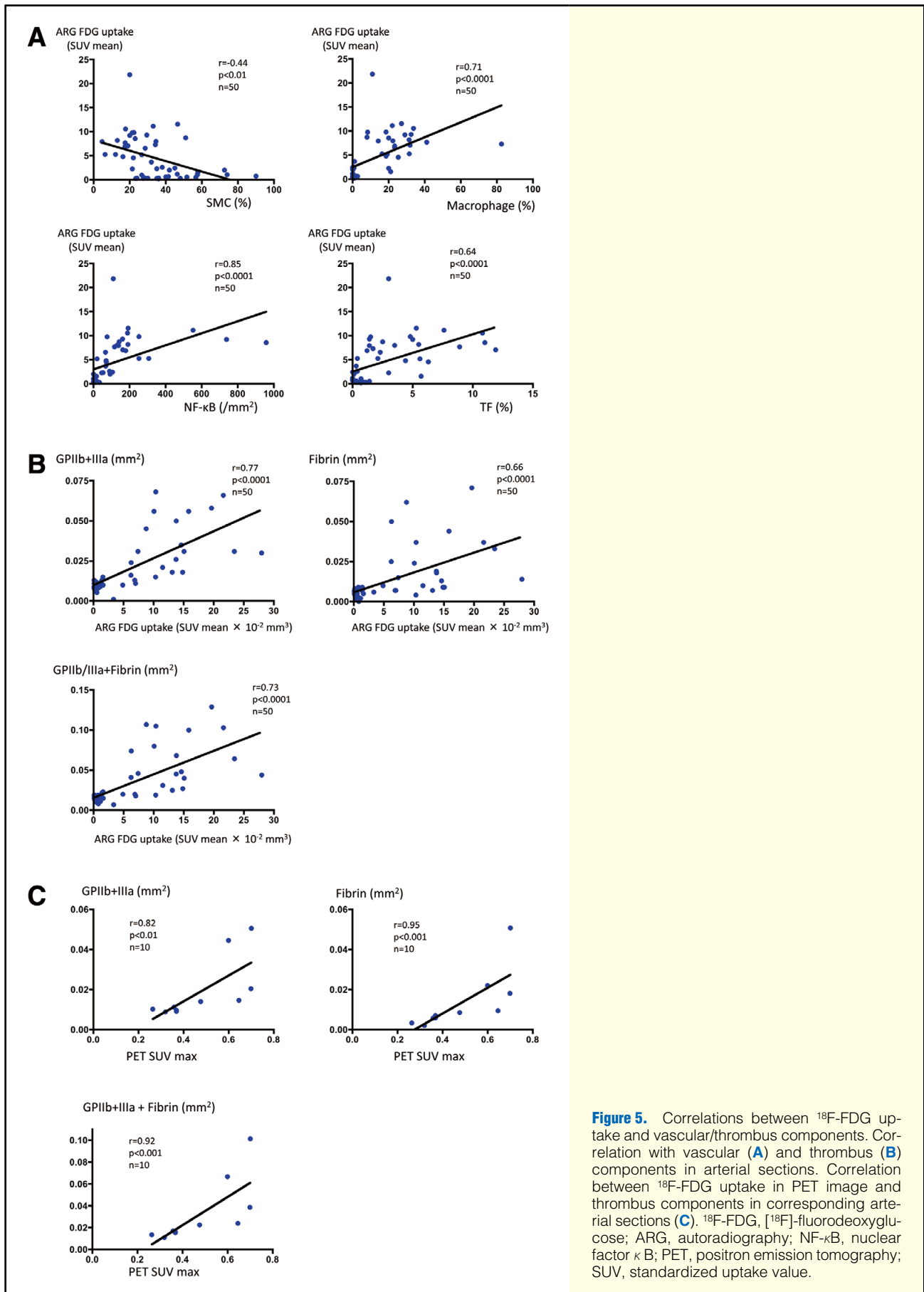
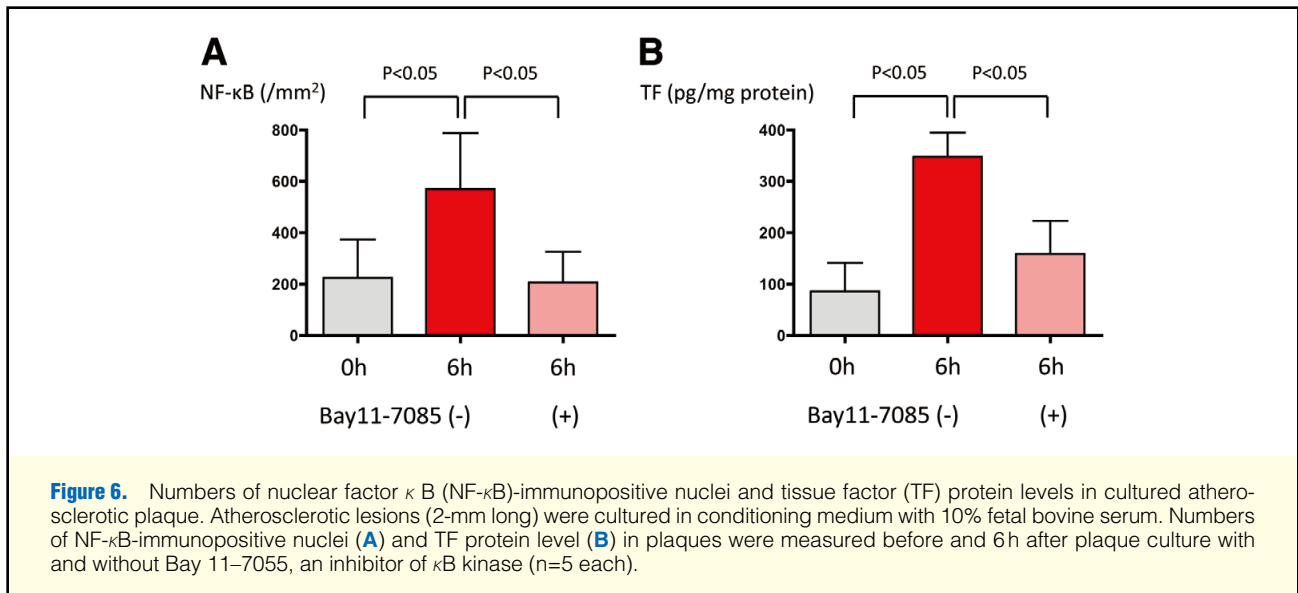


Figure 5. Correlations between ^{18}F -FDG uptake and vascular/thrombus components. Correlation with vascular (**A**) and thrombus (**B**) components in arterial sections. Correlation between ^{18}F -FDG uptake in PET image and thrombus components in corresponding arterial sections (**C**). ^{18}F -FDG, [^{18}F]-fluorodeoxyglucose; ARG, autoradiography; NF- κ B, nuclear factor κ B; PET, positron emission tomography; SUV, standardized uptake value.



cultured plaque tissue.

Arterial ^{18}F -FDG uptake significantly correlated with the size of thrombus induced by balloon injury of the rabbit ilio-femoral artery (**Figure 5B**). A clinical study of patients with atherosclerosis has demonstrated higher ^{18}F -FDG uptake in culprit lesions associated with acute coronary thrombosis than in lesions stented for stable angina.²⁰ Azis et al found significantly more ^{18}F -FDG uptake in rabbit atherosclerotic aortic segments with than without thrombus formation triggered by Russell's viper venom and histamine.¹⁴ Patel et al reported that lowering cholesterol absorption reduces plaque burden, ^{18}F -FDG uptake and thrombus formation in rabbit atherosclerotic aortas, whereas ^{18}F -FDG uptake and macrophage content in the aortas do not correlate.²¹ Those results imply an association between ^{18}F -FDG uptake and thrombogenic factors in the arteries, but the macrophage content does not necessarily correspond to thrombus formation. The present study identified a positive correlation between ^{18}F -FDG uptake and thrombus size, as well as TF expression. In addition, not only the areas of fibrin but also those with platelets correlated with ^{18}F -FDG uptake (**Figures 5A,B**). Because thrombin generated via the TF pathway accelerates platelet activation, as well as fibrin formation,²² evidence of a positive correlation between ^{18}F -FDG uptake and TF expression would support previous findings indicating that ^{18}F -FDG uptake is associated with plaque thrombogenicity.

Although radioactivity in thrombus might affect the correlation between thrombus size and ^{18}F -FDG uptake measured autoradiographically, the amount of radioactivity in the blood and non-injured artery was equally low. Moreover, thrombus size also correlated with ^{18}F -FDG uptake measured by PET imaging (**Figure 5C**). These results suggest that FDG uptake reflects the thrombogenic potential of the arterial wall following balloon injury.

Arterial ^{18}F -FDG uptake significantly correlated with macrophage content (**Figure 5A**). The finding that ^{18}F -FDG uptake positively correlated with this, but negatively with that of SMC, is compatible with those of previous studies.^{8-10,23} Macrophages and granulocytes express glucose transporter 1 and hexokinase II in lung inflammatory lesions. ^{18}F -FDG uptake correlates with the degree of inflammation²⁴ and lipopolysaccharide enhances

^{18}F -FDG uptake by isolated human monocyte-macrophages.²⁵ Therefore, it is considered that ^{18}F -FDG uptake by macrophages is a hallmark of active inflammation in atherosclerotic plaques. However, clinical and experimental studies have failed to show a correlation between ^{18}F -FDG uptake and macrophage content in atherosclerotic lesions.^{21,26} The evidence suggests that the presence of macrophages does not always indicate active inflammation. Recent studies have revealed macrophage heterogeneity in atherosclerotic lesions,²⁷ and approximately 25% of macrophages in coronary atherosclerotic plaques have an antiinflammatory phenotype.²⁸ Moreover, classical but not innate activation significantly increases 2-deoxy-D-glucose uptake, accompanied by glycolytic pathway activation.²⁹ In the present study, CD163-positive cells accounted for only 1% of macrophages in rabbit atherosclerotic artery. The positive relation between ^{18}F -FDG uptake and macrophage content in this model may be related to a paucity of macrophages with an antiinflammatory phenotype (ie, CD163-positive cells) in the rabbit atherosclerotic artery.

The nuclear transcription factor, NF- κ B, affects the inflammatory response, cell proliferation and survival, and angiogenesis in atherosclerotic lesions.³⁰ Activated NF- κ B has been identified in atherosclerotic plaques from humans and in animal models.³¹⁻³³ The expression of NF- κ B in coronary atherosclerotic plaque is more enhanced in patients with unstable than with stable angina pectoris.³⁴ In the present study, immunoreactivity for NF- κ B was distributed predominantly in macrophages and less so in SMCs in atherosclerotic lesions (**Figure 4B**), and there was significant correlation among ^{18}F -FDG uptake, macrophage content, NF- κ B, and TF. These results are compatible with those from a previous report showing colocalization of deoxyglucose and annexin A5, a marker of thrombogenic cell surface, in macrophage-rich atherosclerotic lesions in mice.⁸ These results also suggest that metabolically active cells in the arterial wall have a high-thrombogenic potential in lesions.

TF is upregulated in both human and rabbit atherosclerotic lesions^{4,35} and its expression has been extensively investigated in cultured monocytic cells, SMCs, endothelial cells and fibroblasts.³⁶ Basal and inducible TF expression is regulated by several transcriptional factors, such as Sp1, NF- κ B, EGR-1, and

AP-1. However, its regulatory mechanisms in atherosclerotic plaques are not fully understood. The present study found that TF and NF- κ B-immunopositive areas were similarly distributed, and a tissue culture study of the plaques revealed that inhibiting NF- κ B significantly reduced TF expression (Figures 4,6). These results indicated that NF- κ B mediates TF expression in atherosclerotic plaques. The finding of a positive relationship between ¹⁸F-FDG uptake and arterial thrombus size might be partly explained by TF expression mediated by NF- κ B.

Although a prospective clinical study has not yet examined the predictive value of ¹⁸F-FDG-PET in cardiovascular events, circumstantial evidence has been obtained from a retrospective series of patients with cancer who underwent PET scanning. Paulmier et al reported that extensive arterial ¹⁸F-FDG uptake on PET images might be an indicator of an evolving atherosclerotic process in stable cancer patients.³⁷ Rominger et al also found that increased ¹⁸F-FDG uptake in major arteries emerged as a powerful predictor of subsequent vascular events in a large cohort study of patients with cancer.¹² In addition, a case-control pilot study suggested that arterial ¹⁸F-FDG foci in the aortic arch and carotid bifurcation are associated with a risk of subsequent ischemic stroke.¹³ Those clinical findings suggest that ¹⁸F-FDG-PET can identify patients at risk for future cardiovascular events and the present results support this notion.

The present study did not show balloon catheter-induced thrombus formation in the normal artery of rabbits fed with conventional diet, because we have previously examined balloon catheter-induced thrombus formation in rabbit femoral arteries. The thrombus size in the normal femoral artery was significantly smaller than that in the injured (atherosclerotic) artery in rabbits fed with 0.5% cholesterol diets, and did not differ from that in the femoral artery of rabbits fed with 0.5% cholesterol diet.¹⁵

Study Limitations

The thrombus mechanically induced by a balloon catheter does not replicate spontaneous plaque rupture in human atherothrombosis. Although a recent in vitro study demonstrated that hypoxia augments ¹⁸F-FDG uptake in cultured macrophages,³⁸ we did not assess the contribution of hypoxia to ¹⁸F-FDG uptake in our model. Because thrombus size was evaluated 15 min after its induction, it was not possible to show thrombus persistence and growth rates, both of which are important factors in human atherothrombosis.

Conclusions

Arterial ¹⁸F-FDG uptake is associated with thrombogenic factors and thrombus formation in rabbit atherosclerotic lesions, and arterial ¹⁸F-FDG uptake appears to reflect thrombotic risk of atherosclerotic plaques following balloon injury.

Acknowledgments

The work was supported in part by Grants-in-Aid for Scientific Research in Japan (Nos.23790410 A.Y., 23659573 Y.K., 23390084 Y.A.), Mitsubishi Pharma Research Foundation (A.Y.), and Integrated Research Project for Human and Veterinary Medicine, University of Miyazaki (A.Y., Y.A.), and Project for Developing Innovation Systems from the Ministry of Education, Culture, Sports, Science and Technology, the Japanese Government (N.T.).

Disclosures

Conflict of Interest: We have no conflicts of interest to declare.

References

- Sato Y, Hatakeyama K, Marutsuka K, Asada Y. Incidence of asymptomatic coronary thrombosis and plaque disruption: Comparison of non-cardiac and cardiac deaths among autopsy cases. *Thromb Res* 2009; **124**: 19–23.
- Ueda Y, Ogasawara N, Matsuo K, Hirotsu S, Kashiwase K, Hirata A, et al. Acute coronary syndrome: Insight from angiography. *Circ J* 2010; **74**: 411–417.
- Lee KW, Lip GY. Acute coronary syndromes: Virchow's triad revisited. *Blood Coagul Fibrinol* 2003; **14**: 605–625.
- Drake TA, Morrissey JH, Edgington TS. Selective cellular expression of tissue factor in human tissues: Implications for disorders of hemostasis and thrombosis. *Am J Pathol* 1989; **134**: 1087–1097.
- Hatakeyama K, Asada Y, Marutsuka K, Sato Y, Kamikubo Y, Sumiyoshi A. Localization and activity of tissue factor in human aortic atherosclerotic lesions. *Atherosclerosis* 1997; **133**: 213–219.
- Nicholls SJ, Andrews J, Puri R, Uno K, Kataoka Y. Imaging progression of coronary atherosclerosis. *Circ J* 2012; **77**: 3–10.
- Zagorchev L, Mulligan-Keohoe MJ. Advances in imaging angiogenesis and inflammation in atherosclerosis. *Thromb Haemost* 2011; **105**: 820–827.
- Zhao Y, Zhao S, Kuge Y, Strauss WH, Blankenberg FG, Tamaki N. Localization of deoxyglucose and annexin A5 in experimental atheroma correlates with macrophage infiltration but not lipid deposition in the lesion. *Mol Imaging Biol* 2011; **13**: 712–720.
- Ogawa M, Ishino S, Mukai T, Asano D, Teramoto N, Watabe H, et al. ¹⁸F-FDG accumulation in atherosclerotic plaques: Immunohistochemical and PET imaging study. *J Nucl Med* 2004; **45**: 1245–1250.
- Tawakol A, Migrino RQ, Hoffmann U, Abbara S, Houser S, Gewirtz H, et al. Noninvasive in vivo measurement of vascular inflammation with F-18 fluorodeoxyglucose positron emission tomography. *J Nucl Cardiol* 2005; **12**: 294–301.
- Tahara N, Kai H, Yamagishi S, Mizoguchi M, Nakaura H, Ishibashi M, et al. Vascular inflammation evaluated by [¹⁸F]-fluorodeoxyglucose positron emission tomography is associated with the metabolic syndrome. *J Am Coll Cardiol* 2007; **49**: 1533–1539.
- Rominger A, Saam T, Wolpers S, Cyran CC, Schmidt M, Foerster S, et al. ¹⁸F-FDG PET/CT identifies patients at risk for future vascular events in an otherwise asymptomatic cohort with neoplastic disease. *J Nucl Med* 2009; **50**: 1611–1620.
- Grandpierre S, Desandes E, Meneroux B, Djabballah W, Mandry D, Netter F, et al. Arterial foci of F-18 fluorodeoxyglucose are associated with an enhanced risk of subsequent ischemic stroke in cancer patients: A case-control pilot study. *Clin Nucl Med* 2011; **36**: 85–90.
- Aziz K, Berger K, Claycombe K, Huang R, Patel R, Abela GS. Non-invasive detection and localization of vulnerable plaque and arterial thrombosis with computed tomography angiography/positron emission tomography. *Circulation* 2008; **117**: 2061–2070.
- Yamashita A, Matsuda S, Matsumoto T, Moriguchi-Goto S, Takahashi M, Sugita C, et al. Thrombin generation by intimal tissue factor contributes to thrombus formation on macrophage-rich neointima but not normal intima of hyperlipidemic rabbits. *Atherosclerosis* 2009; **206**: 418–426.
- Zhao S, Kuge Y, Yi M, Zhao Y, Hatano T, Magota K, et al. Dynamic ¹¹C-methionine PET analysis has an additional value for differentiating malignant tumors from granulomas: An experimental study using small animal PET. *Eur J Nucl Med Mol Imaging* 2011; **38**: 1876–1886.
- Aide N, Louis MH, Dutoit S, Labiche A, Lemoisson E, Briand M, et al. Improvement of semi-quantitative small-animal PET data with recovery coefficients: A phantom and rat study. *Nucl Med Commun* 2007; **28**: 813–822.
- Kaim AH, Weber B, Kurrer MO, Gottschalk J, Von Schulthess GK, Buck A. Autoradiographic quantification of ¹⁸F-FDG uptake in experimental soft-tissue abscesses in rats. *Radiology* 2002; **223**: 446–451.
- Neumann RA, Knobler RM, Pieczkowski F, Gebhart W. Enzyme histochemical analysis of cell viability after argon laser-induced coagulation necrosis of the skin. *J Am Acad Dermatol* 1991; **25**: 991–998.
- Rogers IS, Nasir K, Figueroa AL, Cury RC, Hoffmann U, Vermylen DA, et al. Feasibility of FDG imaging of the coronary arteries: Comparison between acute coronary syndrome and stable angina. *JACC Cardiovasc Imaging* 2010; **3**: 388–397.
- Patel R, Janoudi A, Vedre A, Aziz K, Tamhane U, Rubinstein J, et al. Plaque rupture and thrombosis are reduced by lowering cholesterol levels and crystallization with ezetimibe and are correlated with fluorodeoxyglucose positron emission tomography. *Arterioscler Thromb Vasc Biol* 2011; **31**: 2007–2014.
- Crawley JT, Zanardelli S, Chion CK, Lane DA. The central role of

- thrombin in hemostasis. *J Thromb Haemost* 2007; **5**(Suppl 1): 95–101.
23. Davies JR, Izquierdo-Garcia D, Rudd JH, Figg N, Richards HK, Bird JL, et al. FDG-PET can distinguish inflamed from non-inflamed plaque in an animal model of atherosclerosis. *Int J Cardiovasc Imaging* 2010; **26**: 41–48.
 24. Mamede M, Higashi T, Kitaichi M, Ishizu K, Ishimori T, Nakamoto Y, et al. [¹⁸F]FDG uptake and PCNA, Glut-1, and Hexokinase-II expressions in cancers and inflammatory lesions of the lung. *Neoplasia* 2005; **7**: 369–379.
 25. Deichen JT, Prante O, Gack M, Schmiedehausen K, Kuwert T. Uptake of [¹⁸F]fluorodeoxyglucose in human monocyte-macrophages in vitro. *Eur J Nucl Med Mol Imaging* 2003; **30**: 267–273.
 26. Myers KS, Rudd JH, Hailman EP, Bolognese JA, Burke J, Pinto CA, et al. Correlation between arterial FDG uptake and biomarkers in peripheral artery disease. *JACC Cardiovasc Imaging* 2012; **5**: 38–45.
 27. Waldo SW, Li Y, Buono C, Zhao B, Billings EM, Chang J, et al. Heterogeneity of human macrophages in culture and in atherosclerotic plaques. *Am J Pathol* 2008; **172**: 1112–1126.
 28. Boyle JJ, Harrington HA, Piper E, Elderfield K, Stark J, Landis RC, et al. Coronary intraplaque hemorrhage evokes a novel atheroprotective macrophage phenotype. *Am J Pathol* 2009; **174**: 1097–1108.
 29. Tawakol A, Rudd JH, Fayad ZA, Boscá L. Classical but not innate activation augments 2-deoxy-D-glucose uptake in macrophages: Implications for atherosclerosis imaging. *J Nucl Med* 2012; **53**(Suppl 1): 141.
 30. Monaco C, Paleolog E. Nuclear factor kappaB: A potential therapeutic target in atherosclerosis and thrombosis. *Cardiovasc Res* 2004; **61**: 671–682.
 31. Brand K, Page S, Rogler G, Bartsch A, Brandl R, Knuechel R, et al. Activated transcription factor nuclear factor-kappa B is present in the atherosclerotic lesion. *J Clin Invest* 1996; **97**: 1715–1722.
 32. Hajra L, Evans AI, Chen M, Hyduk SJ, Collins T, Cybulsky MI. The NF-kappa B signal transduction pathway in aortic endothelial cells is primed for activation in regions predisposed to atherosclerotic lesion formation. *Proc Natl Acad Sci USA* 2000; **97**: 9052–9057.
 33. Chen H, Yang J, Zhang Q, Chen LH, Wang Q. Corosolic acid ameliorates atherosclerosis in apolipoprotein E-deficient mice by regulating the nuclear factor- κ B signaling pathway and inhibiting monocyte chemoattractant protein-1 expression. *Circ J* 2012; **76**: 995–1003.
 34. Wilson SH, Best PJ, Edwards WD, Holmes DR Jr, Carlson PJ, Celermajer DS, et al. Nuclear factor-kappaB immunoreactivity is present in human coronary plaque and enhanced in patients with unstable angina pectoris. *Atherosclerosis* 2002; **160**: 147–153.
 35. Hatakeyama K, Asada Y, Marutsuka K, Kataoka H, Sato Y, Sumiyoshi A. Expression of tissue factor in the rabbit aorta after balloon injury. *Atherosclerosis* 1998; **139**: 265–271.
 36. Mackman N. Regulation of the tissue factor gene. *Thromb Haemost* 1997; **78**: 747–754.
 37. Paulmier B, Duet M, Khayat R, Pierquet-Ghazzar N, Laissy JP, Maunoury C, et al. Arterial wall uptake of fluorodeoxyglucose on PET imaging in stable cancer disease patients indicates higher risk for cardiovascular events. *J Nucl Cardiol* 2008; **15**: 209–217.
 38. Folco EJ, Sheikine Y, Rocha VZ, Christen T, Shvartz E, Sukhova GK, et al. Hypoxia but not inflammation augments glucose uptake in human macrophages: Implications for imaging atherosclerosis with 18fluorine-labeled 2-deoxy-D-glucose positron emission tomography. *J Am Coll Cardiol* 2011; **58**: 603–614.